Gauge invariance, parton transverse momenta, and single-lepton spectra at high transverse momentum

John F. Gunion
Department of Physics, University of California, Davis, California 95616
(Received 18 February 1976)

We discuss minimal extensions of the Drell-Yan process to low Q^2, incorporating gauge invariance and transverse-momentum fluctuations of the partons. Resulting predictions for single-lepton cross sections at high P_T and for lepton pair production at low Q^2 are discussed. Existing single-lepton spectra with $P_T < 5$ GeV/c are not explained by these extensions of the Drell-Yan process but for $P_T > 5$ GeV/c the Drell-Yan mechanism will probably dominate.

INTRODUCTION

One of the most important tests of the parton model is the power-law scaling predicted for the Drell-Yan annihilation mechanism[1-3] for massive-photon production. This process is only just becoming accessible to experiment.[4] While verification of the scaling is of the most immediate importance, other detailed features, such as the normalization of the cross section, $d\sigma/dQ^2$, and the transverse-momentum distribution $d\sigma/dQ^2dQ_T$ of the massive photon (Q_T is the photon transverse momentum) are also of great interest,[5-7] as they probe the shape and normalization of parton distributions for quarks and antiquarks within hadrons. Predictions for $d\sigma/dQ^2$ in pp collisions have been given using quark distributions extracted[8] from deep-inelastic scattering data, but reliable Q_T dependence estimates do not exist.[9]

This paper will present calculations of $d\sigma/dQ^2dQ_T$ using a framework of quark-counting rules.[10] Corresponding contributions to high-P_T single-lepton production are also presented. Events with low Q^2 and high Q_T might significantly affect, or even dominate, the high-P_T single-lepton spectra.[11-13] Therefore, we have attempted to construct minimal self-consistent extensions of the high-Q^2 annihilation process to the region of low Q^2. In the present calculation, single-lepton production at high P_T tends to arise mainly from high Q^2 but is a factor of 5—10 higher than that calculated ignoring transverse fluctuations in Q_T of the massive photon. For $P_{\rm lab} = 300$ GeV/c the predicted single-lepton cross section is flatter in P_T than the experimental cross section. Since the experimental and theoretical values are approximately the same at the highest measured P_T value of 5 GeV/c one should observe a flattening of the lepton spectrum for $P_T > 5$ GeV/c. The calculations do not explain in any natural way the magnitude of the single-lepton cross section at low P_T. Thus the significant differences between muons and electrons predicted in the present approach at low P_T will not be observable for 0.5 GeV/$c < P_T$. For very small P_T values (< 0.3 GeV/c) both the μ and e Drell-Yan cross sections become quite large and could perhaps be important experimentally though relevant data do not exist. Since the electron cross section is predicted to rise rapidly, as P_T decreases, compared to the μ cross section, a significant μ-e difference could become apparent, experimentally, in this region.

For lower energies significant μ-e differences arise in the model at all $P_T < 2$ GeV/c. The predicted l/π ratios are less than 10^{-4} except at small P_T values. We conclude that other mechanisms are probably required to explain the data.

THEORETICAL CONSIDERATIONS

We first briefly discuss the necessary theoretical ingredients. The naive form for $d\sigma/dQ^2$ in the annihilation model is (see Ref. 5, for example)

$$\frac{d\sigma}{dQ^2dQ_T} = \frac{4\pi\alpha^2}{3Q^2}\,\frac{1}{Q^2}\sum_a \lambda_a^2 \int f_{a/p}(x_a, k_{\perp a}) f_{\bar a/p}(x_{\bar a}, k_{\perp \bar a})\, dx_a dx_{\bar a} d^2k_{\perp a} d^2k_{\perp \bar a}\, \delta((k_a + k_{\bar a})^2 - Q^2)$$
$$\times \delta^2(k_{\perp a} + k_{\perp \bar a} - Q_T)(-\tfrac{1}{4})\,\mathrm{Tr}(\not{k}_a \gamma_\mu \not{k}_{\bar a} \gamma_\mu)\,, \qquad (1)$$

where k_a is the off-shell parton momentum emanating from one incoming proton and $k_{\bar a}$ is that of the antiparton; see Fig. 1. The parton charge is $\lambda_a e$. Parton a carries fraction x_a of its parent proton's incoming momentum and $k_{\perp a}$ is the parton momentum component perpendicular to the direction of that proton. Q_T is the c.m. transverse momentum of the massive photon. The "cores," c_a

and $c_{\bar{a}}$, appear in the final state and hence are on-shell. The energy components of k_a and $k_{\bar{a}}$ are determined by energy conservation. We ignore color which would decrease all results by a factor of 3.

At high Q^2 and s, if we integrate over Q_T and use asymptotic forms for $(k_a + k_{\bar{a}})^2$ and the trace, (1) reduces to the standard Drell-Yan result[1]

$$\frac{d\sigma}{dQ^2} = \frac{4\pi\alpha^2}{3Q^2} \sum_a \frac{\lambda_a^2}{Q^2} \int dx_a\, dx_{\bar{a}}\, x_a f_{a/p}(x_a) x_{\bar{a}} \times f_{\bar{a}/p}(x_{\bar{a}}) \delta(x_a x_{\bar{a}} - Q^2/s). \quad (2)$$

The integration over parton transverse momenta has been absorbed in the definition of the usual distribution function for quarks in a proton, as extracted from deep-inelastic electron-proton and electron-neutron scattering $[\nu W_2^{ep}(x) = \sum \lambda_a^2 x f_{a/p}(x)]$,

$$f_{a/p}(x_a) = \int d^2k_{\perp a} f_{a/p}(x_a, k_{\perp a}). \quad (3)$$

According to the rules of quark counting[7, 8, 14]

$$f_{a/p}(x_a) \underset{x_a \to 1}{\sim} (1 - x_a)^{2N_{a/p} - 3} \quad (4)$$

where $N_{a/p}$ is the number of quarks in the particular proton wave-function component being considered. ($N_{a/p} = 3$ for a "valence" component while $N_{a/p} = 5$ for Regge and Pomeron components.) The corresponding behavior in transverse momentum of the quark is easily obtained[5] using a generalization of quark-counting rules and is

$$f_{a/p}(x_a, k_{\perp a}) = \frac{(2N_{a/p} - 3)}{\pi} \frac{f_{a/p}(x_a)}{(k_{\perp a}^2 + m_{c_a}^2)^{2N_{a/p} - 2}}. \quad (5)$$

Here we have approximated a more general form by a factorized form normalized to reproduce $f_{a/p}(x_a)$ upon integration over $k_\perp$. The core mass m_{c_a} sets the transverse-momentum scale.

By employing various theoretical constraints, including (4), quantum number sum rules, and the deep-inelastic scattering data, quark distributions for each quark type within a proton have been extracted in Ref. 8. Preliminary indications from Fermilab neutrino experiments are that the "sea" or Pomeron so obtained may be somewhat too large, but the situation is far from clear because of anomalies in the y distributions and inconsistencies in the large-x region between neutrino and electron scattering results.[15] Thus we employ the quark distributions of Ref. 8.

At high Q^2 there are no complications and we may employ the above machinery to predict both $d\sigma/dQ^2$ and $d\sigma/dQ^2 dQ_T$. Low-Q^2 predictions require additional model-dependent input as was first stressed in Ref. 3, but they are necessary in order to give a completely self-consistent estimate of single-lepton production. Indeed, as is generally appreciated,[5, 11, 12, 13] there are two extreme ways in which a single lepton may be produced at large transverse momentum, P_T: (i) through the decay of a photon with mass $Q = O(2P_T)$ and (ii) through the decay of a low-mass photon moving with large transverse momentum $Q_T = O(P_T)$. Process (ii) could be significant in comparison to (i) provided the increase in the cross section $d\sigma/dQ^2$ with decreasing Q^2 compensates for the necessity of using photons with large Q_T. In what follows we outline two quite different approaches to the low-Q^2 region.

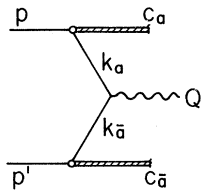

FIG. 1. Drell-Yan annihilation mechanism for photon production.

While there are many physical processes which may be important at low to moderate Q^2 (ψ production, $\rho\omega\phi$ production at high P_T, etc.), our goal here is to consider only those additions to the Drell-Yan model that are absolutely necessary in order to treat this region consistently. Some modification of the naive calculation is necessary since it is only for asymptotic Q^2 that the parton-antiparton annihilation diagram is gauge-invariant on its own. We will consider two extreme ways of guaranteeing gauge invariance of the parton mechanism at any Q^2. The first, I, is *ad hoc*, but is in the spirit of the original model and consists in calculating the annihilation *trace* of Eq. (1) using on-shell parton momenta. The energy component of a parton's momentum used in the trace is determined by the spatial components and the on-shell requirement. Gauge invariance follows immediately.

A physically more realistic approach, II, requires consideration of a bound-state model. A full exploration of such models is beyond the scope of the present work. We adopt a very naive bound-state model which, for the three-quark wave-function component, is consistent with the quark-counting rules of Eqs. (2) and (3), but, for states with more than three quarks, is not.

The model is depicted in Fig. 2. Incoming quarks are treated as weakly bound and share equally the proton's momentum p. The final state consists of a "quark" and a single-particle "core." This simple tree-graph model of scalar partons interacting via ϕ^4 (ϕ^3 in the case of the core) avoids the complexity of loop integrations which would

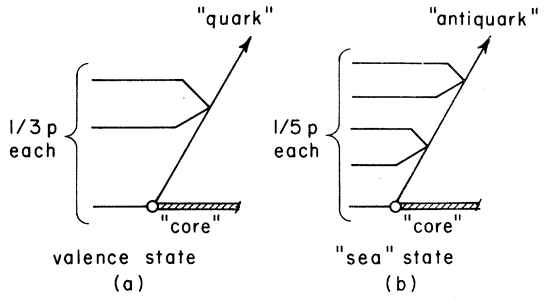

FIG. 2. Our naive model (referred to as II) for valence (a) and sea (b) components of a quark's wave function within the proton.

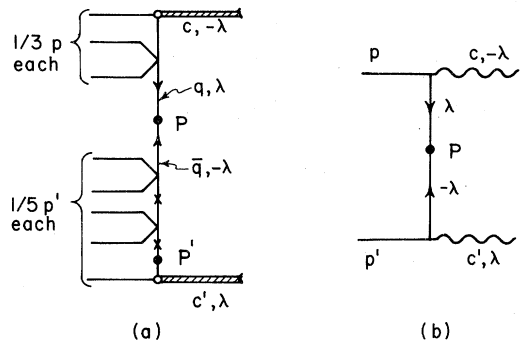

FIG. 3. (a) The skeletal diagram, corresponding to the model of Fig. 2, for proton-proton interaction via joining of q from one proton with $\bar{q}$ from the other. P and P' are two (of many) points of attachment (discussed in the text) for the massive photon. External quarks are chargeless; internal quarks and cores carry charge λ or $-\lambda$; vertices are ϕ^4 or ϕ^3 interactions. (b) A simpler model for proton-proton interactions with a spin-$\frac{1}{2}$ quark and a spin-1 core.

arise if more than a single "core" appeared in the final state aside from the quark. It satisfies the distribution function counting rules in the case of the valence state but has somewhat weaker $(1-x)$ and $k_\perp$ damping than counting rules suggest for a "sea" state. Our goal here, however, is only to gain some idea of the magnitude of corrections to the annihilation diagrams; a complete calculation is clearly a very arduous task.

The resulting picture for the interaction of two protons is given in Fig. 3, illustrating the interaction of a quark, q, from a valence component of one proton with a "sea" quark, $\bar{q}$, of the second proton. We will make the further simplification of treating the incoming quarks as chargeless allowing only the "cores," c and c', and the circulating internal quark to carry charge (λ or $-\lambda$).[16]

The usual Drell-Yan approximation consists of attaching, in Fig. 3, the photon, $\gamma(Q^2)$, at P only. A minimally gauge-invariant calculation requires, in contrast, that $\gamma(Q^2)$ be attached to the circulating charge line at all possible positions. As an example, attachment at P' leads to a contribution to $d\sigma/dQ^2$ which falls like $(1/Q^4)^2$ at high Q^2 (fixed Q^2/s), relative to the annihilation attachment at P. The extra $1/Q^4$ arises from the fact that when $\gamma(Q^2)$ is attached at P' two propagators in Fig. 3 (indicated by x's) are far off-shell $[k^2 = O(Q^2)]$, for large Q^2. When $\gamma(Q^2)$ is attached at P no propagators need be far off-shell.[17,18] This extra contribution is thus negligible for large Q^2 but important and absolutely necessary for gauge invariance at small Q^2.

In summary, we modify the usual Drell-Yan calculation of Eq. (1) by including transverse momentum in the parton distribution functions as described in Eq. (3) and by including corrections required by gauge invariance. Each quark-antiquark annihilation contribution is multiplied by a correction factor generated from the appropriate interaction diagram. For valence-sea annihilation the correction is determined by the complete expression for Fig. 3(a), whereas for sea-sea annihilation a five-quark-on-five-quark skeletal graph is employed.

We stress again that the above model is designed only to provide some idea of the size of corrections to the naive approach, I, which might be expected from a full bound-state model. The variation in results between I and II may reasonably be considered as providing error bars for the calculation of $d\sigma/dQ^2$ at small Q^2. We also mention that one other model has been investigated, namely that based upon the spin-$\frac{1}{2}$ quark skeletal diagram of Fig. 3(b). This model is far from having quark-counting rules incorporated in it yet yields results similar to those from model II.

As we shall see the essential difference between gauge invariance techniques I and II lies in the size of $d\sigma/dQ^2$ at its maximum at small Q^2. The maximum cross section is bigger for case II than for case I. High-P_T single-lepton production remains relatively insensitive to the low-Q^2 region but low-P_T single-lepton cross sections especially at low overall c.m. energy are strongly influenced by the low Q^2 cross section.

RESULTS

We now discuss the results of our calculations. These were performed using a computer program which includes all phase-space and threshold effects related to finite final state particle masses. In model II, the proton mass was chosen for each core and one-third the proton mass was chosen for the internal quarks. Results are very insensitive to these choices. The calculated cross sections are displayed in a series of figures beginning with Fig. 4.

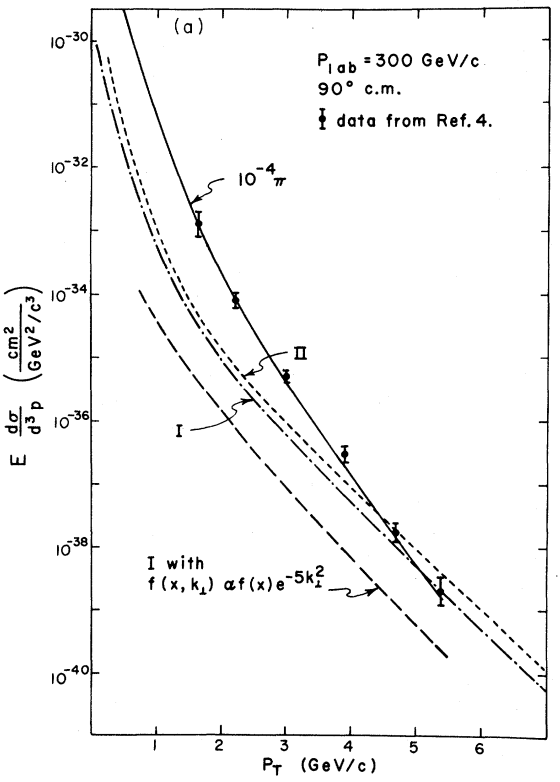

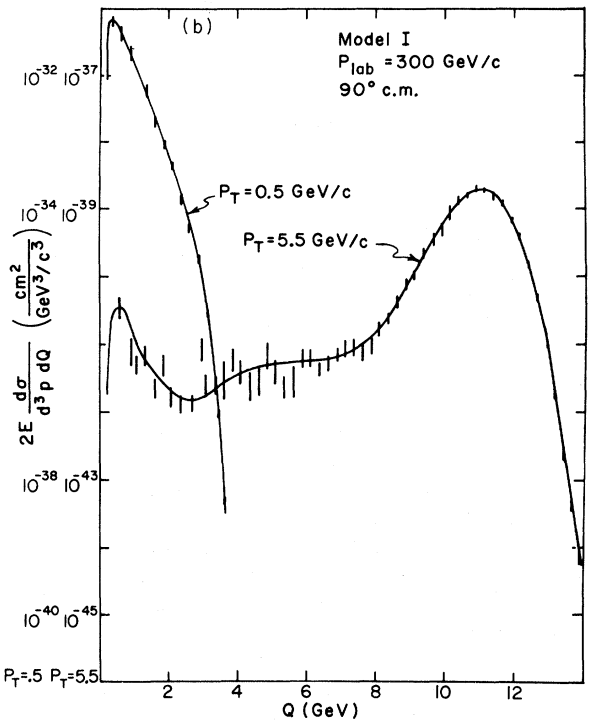

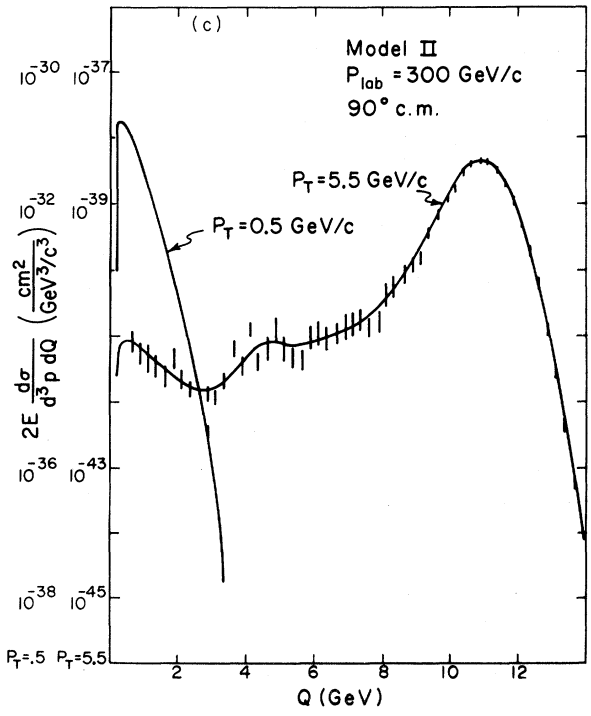

FIG. 4. (a) $E(d\sigma/d^3p)[pp \to \mu(P_T)+X]$ at P_{lab} = 300 GeV/c 90° center of mass (c.m.) calculated in models I and II. P_T is the muon transverse momentum. Also plotted are the existing data and an approximate representation of them, namely, $10^{-4}\times E(d\sigma/d^3p)(pp \to \pi+X)$. Results of a limited-transverse-momentum calculation in model I (little different from ignoring quark transverse momenta) are shown. General note: Some of the graphical plots of computer calculations based on the theoretical models discussed in the text show error bars. These are always indicated by a single vertical bar (or a dashed vertical bar) and simply indicate the program's estimated integration error. When not indicated integration-error estimates were negligible.

(b) $2E(d\sigma/d^3p\,dQ)[pp \to \mu^+\mu^-(Q)+X']$, $\mu^-(P_T)+X$

P_{lab} = 300 GeV/c 90° c.m. Calculated in model I for P_T = 0.5 GeV/c and P_T = 5.5 GeV/c. (c) Same as for (b) but for model II.

μ production

Figure 4(a) shows the predicted spectra $Ed\sigma/d^3p$ $[pp \to \mu(P_T)+X]$ for single-muon production at 90° in the center of mass for a beam momentum of 300 GeV/c. For comparison 10^{-4} times the pion spectrum is plotted. Both models I and II fall below the curve $10^{-4}\times\pi$ at low P_T but cross it near $P_T = 5$ GeV/c. Model II predicts a slightly higher cross section than I at all P_T. Also shown is the result of a calculation using model I but with transverse momenta of the pions severely limited by replacing (3) by

$$f(x, k_\perp) \propto f(x) e^{-5k_\perp^2} \ .$$

The resulting spectrum is approximately a factor of 10 below that including transverse fluctuations according to (3).

Figure 4(b) shows the composition in Q for model I, i.e., $2E(d\sigma/d^3pdQ)[pp \to \mu^+\mu^-(Q)+X \to \mu(P_T)+X]$ for single-lepton production (at 300 GeV/c beam momentum) at two representative P_T values, 0.5 and 5.5 GeV/c. The computer results were not infinitely accurate as indicated by the error bars in this and other graphs.

Figure 4(c) gives the same for model II. In both cases it is clear that at $P_T = 5.5$ GeV/c the major cross-section contributions come from $Q = O(2P_T)$. This means that the small Q^2 photons have too sharp a dropoff in Q_T of the photon to be a major factor in this region. This is illustrated in Fig. 5.

Figure 5(a) plots $(d\sigma/dQ)[pp \to \mu^+\mu^-(Q)+X]$ for model I, $p_{\rm lab} = 300$ GeV/c (and 29.5 GeV/c) and Fig. 5(b) does the same for model II. Note that the small-Q maxima are roughly a factor of 10 higher than those of I while at large Q both models give essentially the same cross section. In Fig. 5(a) we also give the experimental points of the original experiment at 29.5 GeV/c (See Lederman, Ref. 4) modified by the ψ subtraction and linear, A dependence.[4] Agreement at low Q^2 is clearly good. (Strictly speaking, one should compare to curves which include the apparatus acceptance; the numerical effect is to reduce the theoretical curve by a factor of 2.) The near agreement at small Q^2 of experiment and theory is surprising since other physical sources for low-mass photons certainly exist (model II is one simplistic approach which predicts an excess over the naive annihilation result for $Q < 2$ GeV). Perhaps this indicates that the factor of $\frac{1}{3}$ reduction, in the cross sections presented, which results from the effects of color should be incorporated. At large Q, in comparison, even with resonances subtracted, the annihilation model does not seem able to account for the magnitude of the cross section estimated from the 29.5-GeV/c experiment. It is difficult, in the above, to know how reliable Lederman's[4] ψ-resonance subtractions are. A low-Q 250-GeV/c point (quoted in Ref. 4) is also given and appears to be somewhat above the predicted value.

Figure 5(c) plots $(d\sigma/dQ^2dQ_T)[pp \to \mu^+\mu^-(Q, Q_T)+X]$ for model I at $P_{\rm lab} = 300$ GeV/c for a value of Q^2 (0.09 GeV^2) near the maximum in $d\sigma/dQ$ (also for $Q^2 = 16$ GeV^2). At the small value of Q^2, $d\sigma/dQ^2dQ_T$ falls off by a factor of 10^{-9} by $Q_T = 5.5$ GeV/c while $d\sigma/dQ$[Fig. 5(a)] falls by only (roughly) 10^{-7} by $Q = 11$ GeV from its maximum near $Q^2 = 0.09$ GeV^2. Thus lepton production at $P_T = 5.5$ GeV/c will be dominated by the large-Q region, as revealed in Fig. 4, in the present model. This same pattern is repeated for model II. For both I and II the moderately steep falloff in Q_T at small Q^2 is a result of the fairly steep falloff in $k_\perp$ of the "sea" distribution functions, $\propto 1/(k_\perp)$.[16] At small Q^2 sea-sea annihilations dominate and the resulting Q_T spectrum is considerably sharper than at higher Q^2, where valence sea annihilations become important.

The difference in the single-lepton spectra (at least at high P_T) predicted by I and II thus does not arise from the differences in $d\sigma/dQ$ at small Q, but rather from a slightly greater breadth in Q_T at large Q^2 of $d\sigma/dQ^2dQ_T$ for model II.

Figure 6(a) gives $Ed\sigma/d^3p$ for a single muon at $P_{\rm lab} = 29.5$ GeV/c 90°$_{\rm c.m.}$, predicted by models I and II. The low-P_T values plotted are sensitive to low Q^2 and thus II predicts a higher cross section than I, but both are a factor of 10 or more below the comparison of 10^{-4} times the pion spectrum which is probably the approximate experimental cross section (Ref. 4).

Figure 5(e) which plots $d\sigma/dQ^2dQ_T$ from model I for two Q^2 values at $P_{\rm lab} = 29.5$ GeV/c shows that for $Q^2 = 0.0625$ GeV^2 $d\sigma/dQ^2dQ_T$ has fallen by 10^{-10} by $Q_T = 3$ GeV while, from Fig. 5(a), $d\sigma/dQ$ has fallen also by 10^{-10} by $Q = 6$. Thus, as an example, $Ed\sigma/d^3p$ at $P_T = 3$ GeV/c, $P_{\rm lab} = 29.5$ GeV/c will receive important contributions from the entire spectrum of Q^2. This general feature is borne out in Fig. 6(b) which gives Q compositions for $P_T = 1$ and 2.5 GeV/c of the single-lepton spectra at $P_{\rm lab} = 29.5$ GeV/c for model I. The analogous results for model II at $P_{\rm lab} = 29.5$ GeV/c show only minor differences.

Finally, in order to gain a slightly better picture of the $P_{\rm lab}$ dependence of the single-lepton spectrum we plot in Fig. 7 the results for model I at $P_{\rm lab} = 29.5$, 150, and 300 GeV/c and give an approximate fit.

μ-e pair production comparison

We turn now to a discussion of the differences between μ and e pair production predicted by mo-

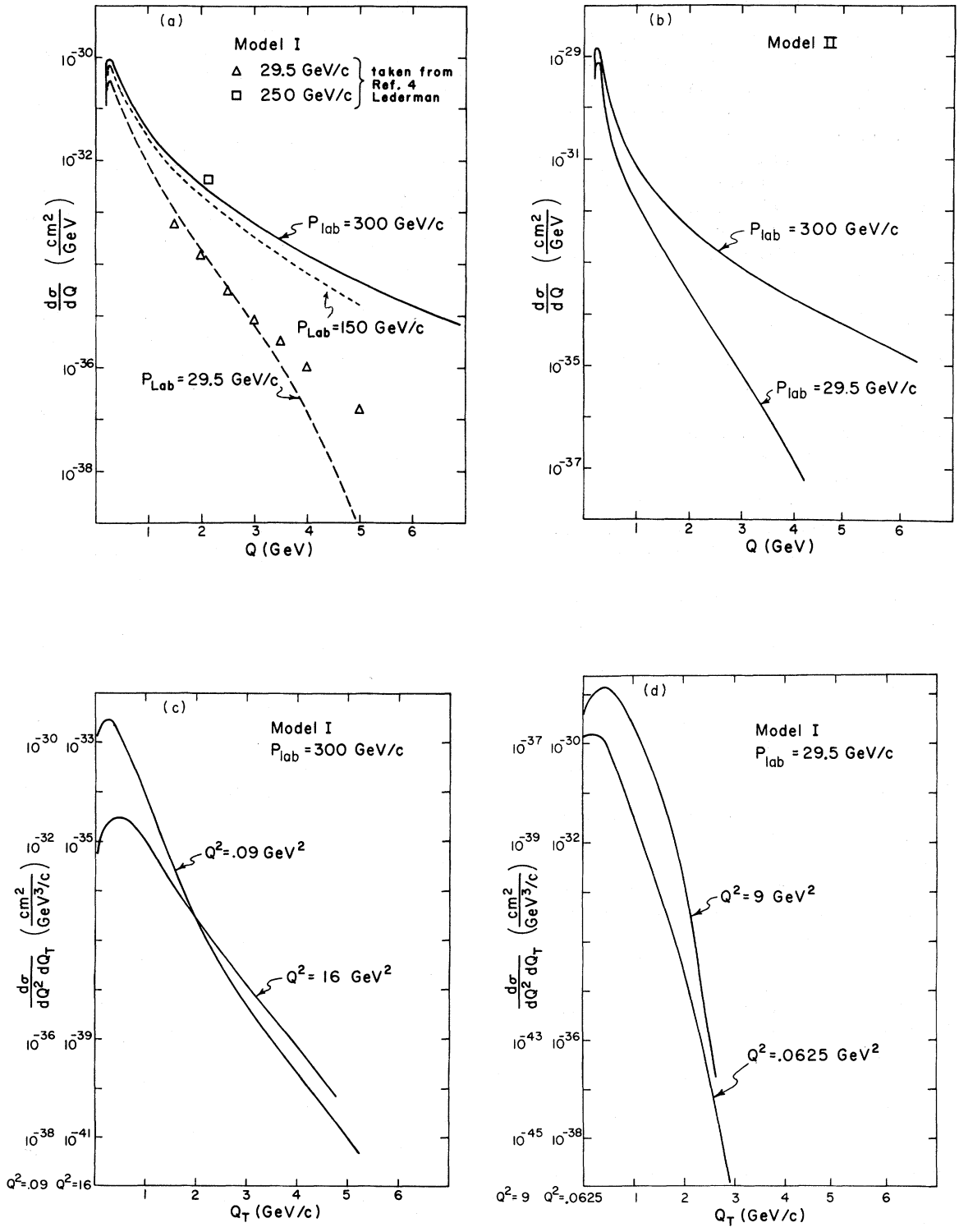

FIG. 5. (a) $(d\sigma/dQ)[pp \to \mu^+\mu^-(Q)+X]$ calculated in model I at three P_{lab} values. (b) Same as for (a) but using model II and only two P_{lab} values. (c) $(d\sigma/dQ^2dQ_T)[pp \to \mu^+\mu^-(Q, Q_T)+X]$, where Q_T is the c.m. transverse momentum of the lepton pair relative to the beam direction. Plots for two Q^2 values are presented at $P_{\text{lab}}=300$ GeV/c for model I. (d) Same as for (c) but with $P_{\text{lab}}=29.5$ GeV/c.

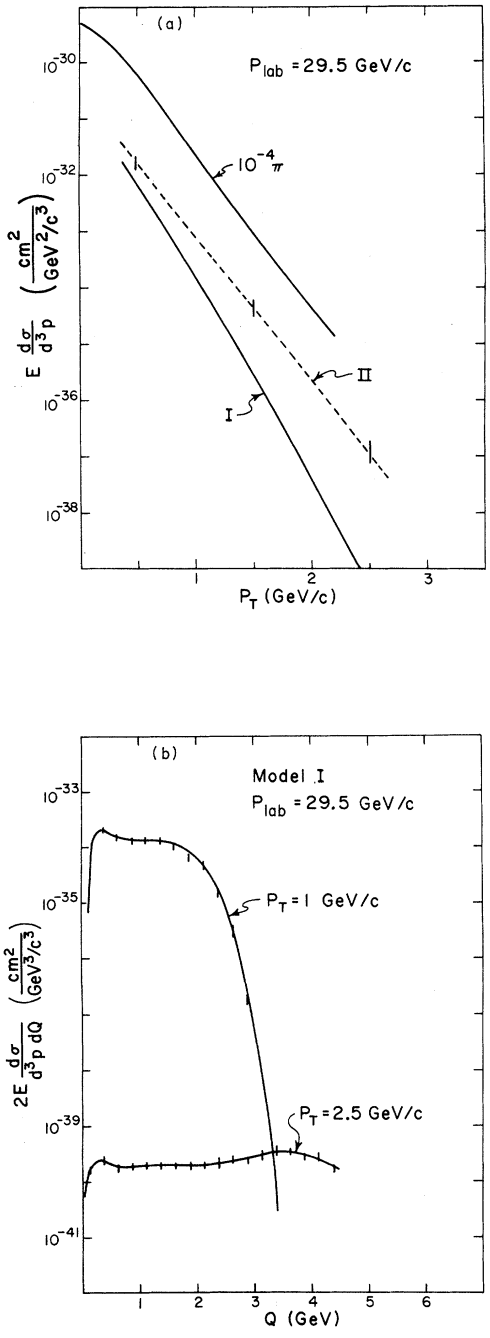

FIG. 6. (a) $E(d\sigma/d^3p)[pp \to \mu^+\mu^-(Q)+X]$
$\hookrightarrow \mu(P_T)+X'$
at P_{lab} = 29.5 GeV/c. Calculations for models I and II are presented and compared to 10^{-4} times the pion spectrum at that energy.

(b) $(2Ed\sigma/d^3p\,dQ)[pp \to \mu^+\mu^-(Q)+X]$
$\hookrightarrow \mu(P_T)+X'$
at P_{lab} = 29.5 GeV/c. Calculations are for model I.

dels I and II. We begin by discussing the $d\sigma/dQ$ and $d\sigma/dQ^2dQ_T$ spectra.

Figure 8(a) compares $d\sigma/dQ$ for μ and e production at P_{lab} = 300 GeV/c and 29.5 GeV/c. The pattern is obvious, $d\sigma/dQ$ for e production is simply a continuation to smaller Q values of the μ pair spectrum with the threshold at $Q = 2m_\mu$ removed. The ultimate maximum of $d\sigma/dQ$ is thus some three orders of magnitude higher for e pairs than for μ pairs.

Figure 8(b) presents the analogous plots for model II. There the ultimate $d\sigma/dQ$ maximum is eight orders of magnitude higher for e pairs than for μ pairs.

One might, on this basis, expect model II to predict a much larger single-e cross section than model I. This is not the case except in the very-small-P_T region because the big difference between $d\sigma/dQ$ for model I and model II arises entirely from the region $Q_T < 0.25$. One other feature which one discovers is that the large-Q_T tail of these small-Q^2 cross sections is actually smaller in magnitude for model II than for model I especially at P_{lab} = 29.5 GeV/c. This is reflected in the single-lepton spectra which we discuss next.

Figure 9(a) presents the μ-e comparison for the single-lepton spectrum at P_{lab} = 300 GeV/c 90° c.m.

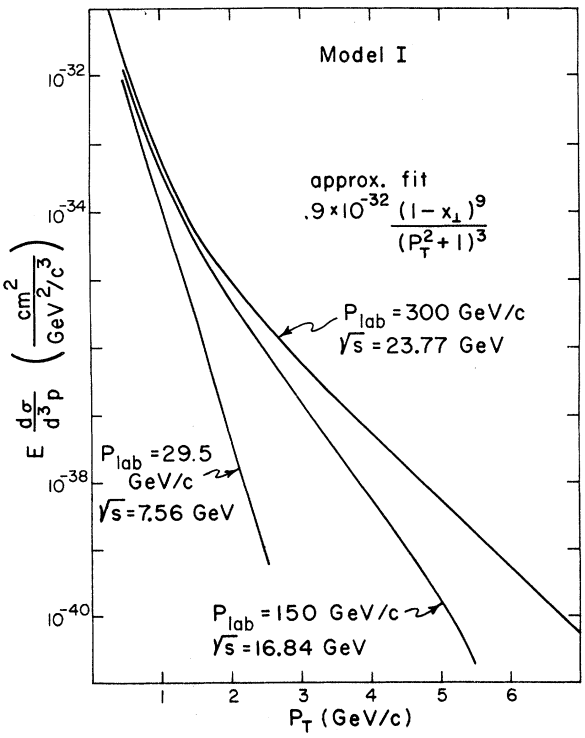

FIG. 7. $E(d\sigma/d^3p)[pp \to \mu(P_T)+X]$ in model I at three P_{lab} values.

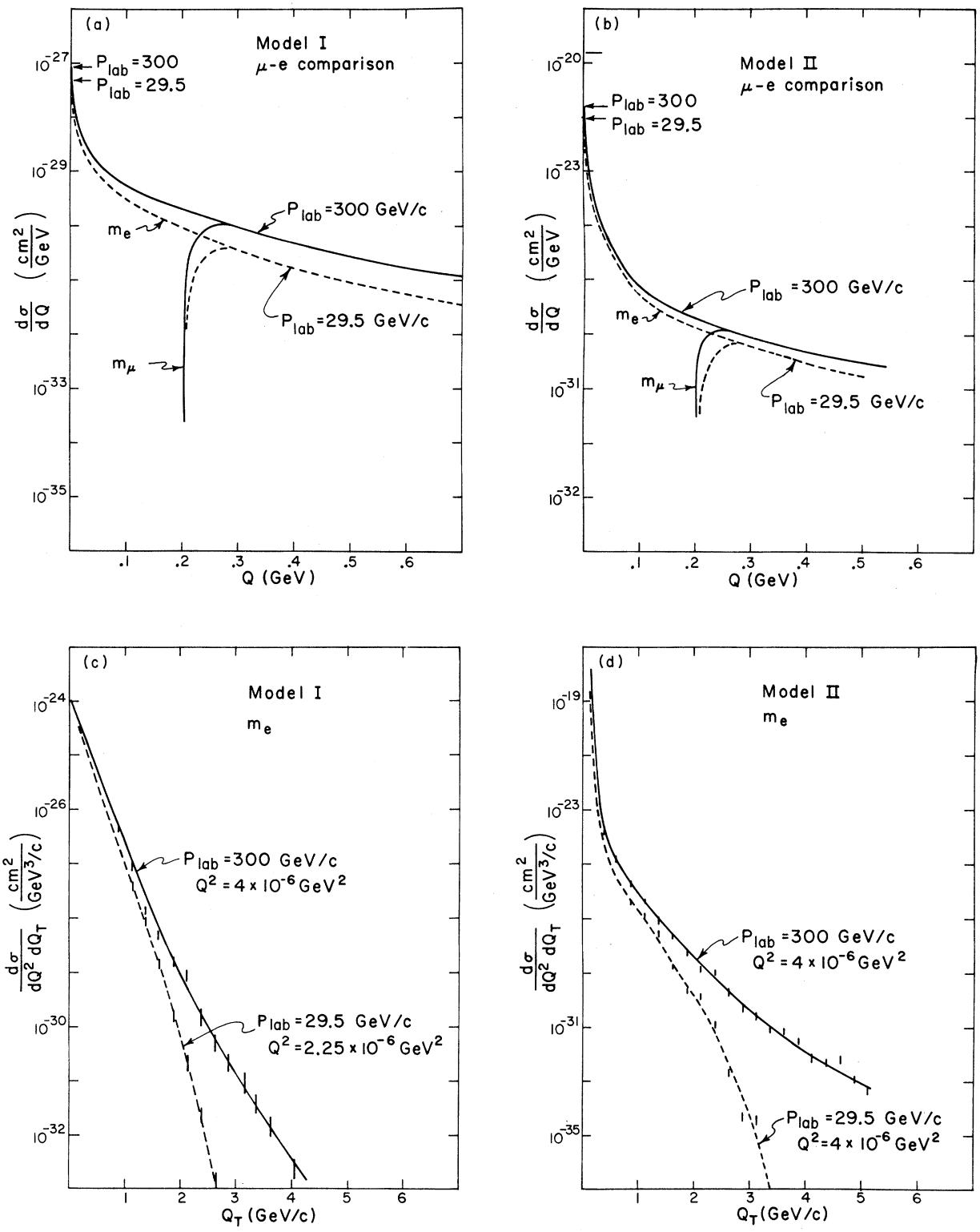

FIG. 8. (a) Comparison of $(d\sigma/dQ)[pp \to l^+l^-(Q) + X]$ for $l = \mu$ vs $l = e$ calculated in model I at $P_{\text{lab}} = 29.5$ GeV/c and 300 GeV/c. (b) Same as for (a) but in model II. (c) $(d\sigma/dQ^2 dQ_T)[pp \to e^+e^-(Q, Q_T) + X]$ in model I for $P_{\text{lab}} = 300$ GeV/c and $P_{\text{lab}} = 29.5$ GeV/c and for Q^2 values near the peak in $d\sigma/dQ$ at these same incident beam momenta. (d) Same as for (c) but using model II.

for model I. Clearly at high P_T there is no μ-e difference whereas at low P_T the e cross section given by our minimal parton model is substantially bigger than the μ cross section though still below the comparison curve $10^{-4}\times\pi$ for $P_T > 0.5$ GeV/c.

Figure 9(b) presents this same comparison for $P_{\text{lab}} = 29.5$ GeV/c. The electron cross section is substantially larger than the muon cross section out to $P_T = 2.5$. Thus for moderately low P_T values, especially at lower energies, the single-electron spectrum makes use of the much larger maximum in $d\sigma/dQ$ compared to the muon case. At high P_T, on the other hand, the large-Q_T tail of the small-Q^2 maximum is ineffective. The composition in Q is illustrated in Fig. 9(c).

Figure 9(c) compares $2Ed\sigma/d^3pdQ$ ($P_{\text{lab}} = 300$ GeV/c at $P_T = 0.5$ GeV/c and 5.5 GeV/c predicted in model I for μ vs e pairs. At $P_T = 0.5$ the major e-spectrum contribution comes from $Q < 2m_\mu$. (This same feature holds also for $P_T < 2.5$ at $P_{\text{lab}} = 29.5$ GeV/c).

At $P_T = 5.5$ there is some small enhancement at small Q in $2Ed\sigma/d^3pdQ$ for e vs μ, but the small-Q region is dominated by the large-Q contributions plotted earlier in Fig. 4(b). The single-lepton μ-e comparisons for model II at $P_{\text{lab}} = 300$ GeV/c and 29.5 GeV/c are similar. As hinted earlier the only surprise is that the electron spectra for model II are below those for model I (just discussed) despite the higher $d\sigma/dQ$ maxima. As mentioned, this is because of the much sharper Q_T falloff in $d\sigma/dQ^2dQ_T$ for model II compared to model I.

CONCLUSIONS

Minimal extensions of the Drell-Yan mechanism to an exactly gauge-invariant model appear incapable of yielding small-Q^2 cross sections with a sufficiently large Q_T tail that small Q^2 can become important in production of a single lepton at high P_T(> 4 GeV/c). Nonetheless the large-P_T single-lepton cross sections which arise from high Q^2 in the models employed and which incorporate fluctuations of the partons are comparable to the data at $P_T = 5$ GeV/c, $P_{\text{lab}} = 300$ GeV/c and should result in a flattening in the spectrum $Ed\sigma/d^3p$ at higher P_T values. (Plots presented ignore color which would lead to a factor 3 decrease in all cross sections presented.) In this region it is especially important to measure $Ed\sigma/d^3pdQ$(where Q is the mass of the lepton pair from which the single lepton originated—assuming photons to be the source of single leptons) to see if it corresponds to the expectations of the parton model. It is also of great interest, as stressed in Ref. 5 and here, to measure $d\sigma/dQ^2dQ_T$ (Q = lepton-pair mass, Q_T = lepton pair transverse momentum). This is especially true at large Q where the Drell-Yan annihilation graph dominates over other terms necessary for gauge invariance and the Q_T distribution directly probes the parton transverse-momenta distributions.

Single-lepton spectra at low P_T and $d\sigma/dQ$ at low Q are much more model-dependent. We have presented calculations for two models which yield quite different results, for instance, for $d\sigma/dQ$ which can be very large at small Q. Model II predicts a cross section a factor of 10 above the naive model I. This enhancement is not unlike that suggested in Ref. 13, but in our case it does not significantly affect single-lepton spectra owing to the very steep falloff in Q_T of $d\sigma/dQ^2dQ_T$ at small Q. Such a steep falloff may be a characteristic feature of many mechanisms which enchance $d\sigma/dQ$ at low Q. In our case it occurs because the asymptotically nonleading contributions become important only when the extra propagators, proportional to $1/Q^2$ (crudely), become large at small Q^2. However, a typical propagator of this type also includes terms sensitive to the off-shell quark momenta. At small Q^2 these can dominate the propagator so that if the $k_\perp$ of the quark is large (in order to yield large Q_T) the quark is generally far enough off-shell to obscure the enhancement. In either case after integrating over all Q^2 values the predicted single-lepton cross sections are too small, at low to moderate P_T, to explain the data. At very small P_T (< 0.3 GeV/c) the single-lepton cross sections predicted by Drell-Yan mechanisms rise dramatically and could become significant experimentally, though relevant data do not exist. The present models suggest the possibility of a large e/μ ratio, in this very-low-P_T region, due simply to the much larger peak value of $d\sigma/dQ^2$ in the electron case. However, this large e/μ ratio may also be present for other types of mechanisms for small-Q^2 lepton pairs. Only absolute cross-section predictions will be able to discriminate among various possible low-mass pair production processes.

The two models employed here are minimal extensions of the Drell-Yan model and do not incorporate other physical processes such as $\rho\omega\phi\psi$ production. Calculations of these, as reviewed in Ref. 4, in combination with the single-lepton cross section calculated here for the purely parton-model mechanisms do not appear adequate to explain the single-lepton spectra observed experimentally. However, this conclusion is dependent on the models employed. For instance, it has been pointed out[19] that, given the limited available information on ψ production, a cross-section form, which fits available data, may be assumed, that provides all of the observed single

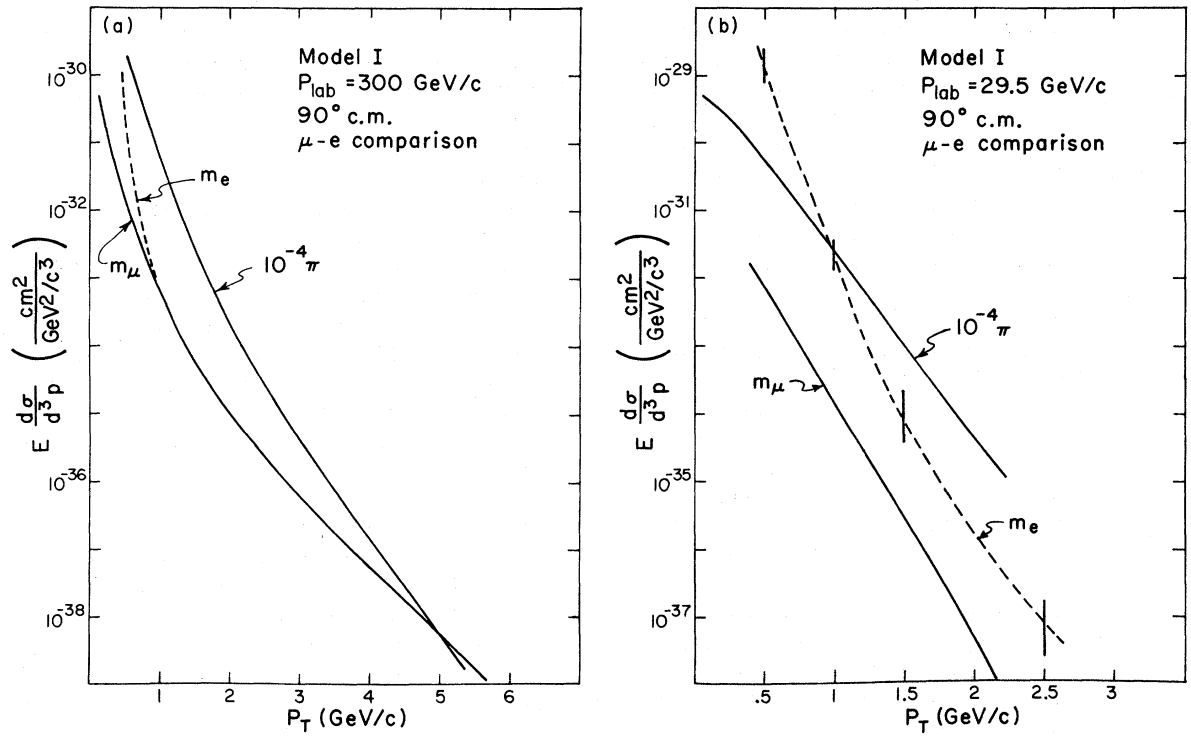

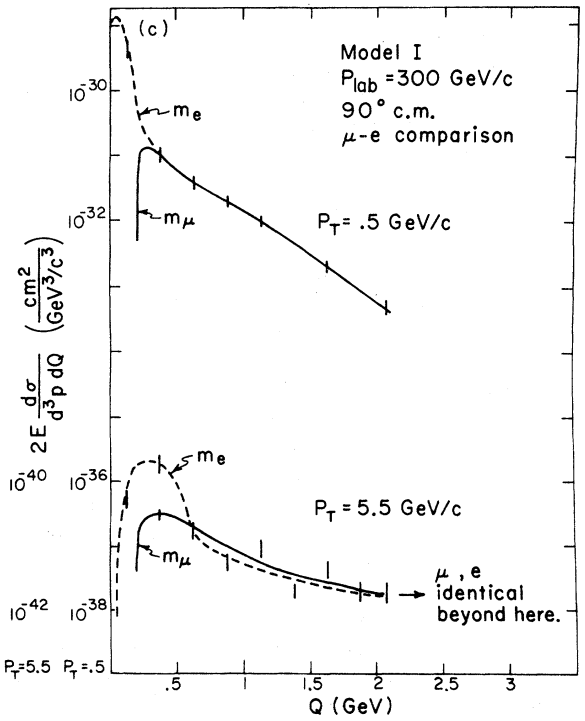

FIG. 9. (a) $E(d\sigma/d^3p)[pp \to l(P_T)+X]$ at P_{lab} = 300-GeV/c 90° c.m. Calculations for model I are compared for $l=\mu$ vs $l=e$. Also the standard curve $10^{-4}\times E(d\sigma/d^3p)[pp \to \pi(P_T)+X]$ is plotted. (b) Same as for (a) but at P_{lab} = 29.5 GeV/c.

(c) $2E(d\sigma/d^3p\,dQ)[pp \to l^+l^-(Q)+X]$

$\searrow l(P_T)+X'$

at P_{lab} = 300 GeV/c 90° c.m. Results for model I at P_T = 0.5 GeV/c and 5.5 GeV/c are presented. At P_T = 5.5 GeV/c the μ and e cross sections are identical beyond $Q=2$. [See Fig. 4(b).] Results for model II are entirely similar in appearance.

leptons at high P_T. This has been confirmed at one energy and for 1.5 GeV/c < P_T < 4.5 GeV/c by recent experimental results of Lederman and collaborators.[19] Thus experimental information on, or model-dependent estimates of, the distribution of $\rho\omega\phi\psi\ldots$ in transverse momentum are clearly vital to reliable estimates of single-lepton cross sections.

Recent results at P_{lab} = 400 GeV/c of Adair *et al.*[20] provide an additional constraint. For instance, our model I predicts an integrated cross section $\int(d\sigma/dQ)dQ$, of roughly 4 μb vs the above experimental result of about 8 μb. In our approach the single-μ spectrum demands that the difference be made up by low-Q^2 lepton pairs with a significant high-Q_T tail. We await anxiously a comprehensive set of measurements of $d\sigma/dQ^2dQ_T$ so that the situation may be clarified. However, it is clear that parton annihilation cross sections are not orders of magnitude below the $d\sigma/dQ$ data.

I would like to acknowledge the important contribution of G. Chu and M. Duong-Van, who provided me with an integration program capable of accurately handling the theoretical model calculations. I would also like to thank S. J. Brodsky, G. Chu, and M. Duong-Van for several helpful conversations.

---

[1]S. D. Drell and T.-M. Yan, Ann. Phys. (N.Y.) 66, 578 (1971).

[2]J. Kuti and V. Weisskopf, Phys. Rev. D 4, 3418 (1971).

[3]P. Landshoff and J. C. Polkinghorne, Nucl. Phys. B33, 221 (1971).

[4]For a review see J. W. Cronin's lecture at Erice School of Subnuclear Physics, 1975 (unpublished) or the talk by L. Lederman, in *Proceedings of the 1975 International Symposium on Lepton and Photon Interactions at High Energies, Stanford, California,* edited by W. T. Kirk (SLAC, Stanford, 1976), p. 265. The 250-GeV/c point analyzed in this latter reference is taken from the data of W. Lee *et al*. (unpublished).

[5]G. Chu and J. F. Gunion, Phys. Rev. D 10, 3672 (1974). The importance of Q_T dependence is stressed in this reference.

[6]H. Paar and E. Paschos, Phys. Rev. D 10, 1502 (1974), discuss $d\sigma/dQ^2$ using distribution function forms which fit deep-inelastic data but are not consistent with quark counting (see Ref. 7).

[7]G. Farrar, Nucl. Phys. B77, 429 (1974), discusses $d\sigma/dQ^2$ within a quark-counting (see Ref. 10) framework and gives single-lepton cross sections ignoring transverse fluctuations.

[8]The distributions employed in this paper are those of J. F. Gunion, Phys. Rev. D 10, 242 (1974). See also Ref. 5; G. Farrar, Ref. 7, also obtains very similar distributions.

[9]Earlier calculations ignore the transverse-momentum fluctuations of the partons stressed in Ref. 5.

[10]S. J. Brodsky and G. Farrar, Phys. Rev. Lett. 31, 1153 (1973). Detailed applications to quark distributions appear in Refs. 8, 7, and 5.

[11]This is implicit in the work of G. Chu and J. Koplik, Phys. Rev. D 11, 3134 (1975).

[12]M. Duong-Van, SLAC Report No. SLAC-PUB-1604 (unpublished).

[13]J. D. Bjorken and H. Weisberg, Phys. Rev. D 13, 1405 (1976).

[14]S. J. Brodsky and R. Blankenbecler, Phys. Rev. D 10, 2973 (1974).

[15]Indeed, at large x, where valence quarks should dominate, one should have

$$\frac{[d\sigma^{\nu N}(x)/dx]}{\nu W_2^{e(p+n)/2}(x)} \approx \tfrac{18}{5}\cos^2\theta_C ,$$

where x is the usual Bjorken variable, $x = (2M\nu/Q^2)^{-1}$, and θ_C is the Cabibbo angle. This ratio which is predicted above to be 3.4 is experimentally ≈ 2. [For a recent review of the data see the *Proceedings of the 1975 International Symposium on Lepton and Photon Interactions at High Energies, Stanford, California,* edited by W. T. Kirk (SLAC, Stanford, 1976).] This anomaly at large x which indicates that $d\sigma^{\nu N}/dx$ is *smaller* than expected is exceedingly difficult to interpret theoretically.

[16]Again this is done to avoid complications which can only be treated correctly in a complete bound-state model. In general our model has photon attachments to the incoming on-shell quarks if charged. However, these produce enhancements in $d\sigma/dQ^2$, at small Q^2, due to the fact that the quark emitting the photon may, for some regions of phase space, be nearly on-shell after the emission. However, in a full bound-state model the incoming quarks would not be exactly on-shell, but would have arisen from a component of the proton's Bethe-Selpeter-type wave function. The diagrams, so generated, represent parton rescattering corrections to the diagrams we consider. I thank S. J. Brodsky for a discussion on this point. The graphs we are discussing here are the parton-model analog of the model considered by S. M. Berman, D. Levy, and T. Neff, Phys. Rev. Lett. 23, B63 (1969). Of course at very low Q the model of Berman *et al*. is appropriate because the interaction with the photon depends only on the total incoming charge according to standard low-energy theorems.

[17]Various types of asymptotically nonleading terms have also been discussed by C. T. Sachrajda and R. Blankenbecler, SLAC Report No. SLAC-PUB-1658 (unpublished), within a quark-counting framework. The model of the text determines the relative normalization of its competing processes on the basis of gauge invariance. See also the specific calculations of M. Fontannaz [Phys. Rev. (to be published)] based on the $qM \to q\gamma$ subprocesses.

[18]Radiative corrections have also been discussed by I. Halliday, Nucl. Phys. B103, 343 (1976).

[19]F. Halzen and K. Kajantie, Phys. Lett. 57B, 361 (1975). Of course, papers by G. Farrar and R. Field [*ibid*. 58B, 80 (1975)] and by M. Bourquin and J.-M. Gaillard [*ibid*. 59B, 191 (1975)] reach the opposite conclusion. More

recently L. Lederman [in Proceedings of the International Storage Ring Meeting, 1976 (unpublished)] has concluded that his measured ψ-production P_T dependence *is* such as to explain the 300-GeV/c single-muon spectrum for 1.5 GeV/$c < P_T < 4.5$ GeV/c.

[20]R. K. Adair, BNL Symposium on Charm and Direct Lepton Production (unpublished).